ISSN 1674-1056
http://cpb.iphy.ac.cn
http://iopscience.iop.org/cpb
中国物理 B
Chinese Physics
中国物理
Chinese Physics B

Hydrogenated antimonene as quantum spin Hall insulator: A first-principles study

Xin He(贺欣), Ji-Biao Li(李佶彪)

Citation: Chin. Phys. B . 2019, 28(3): 037301. **doi:** 10.1088/1674-1056/28/3/037301
Journal homepage: http://cpb.iphy.ac.cn; http://iopscience.iop.org/cpb

What follows is a list of articles you may be interested in

Electric field manipulation of multiple nonequivalent Dirac cones in the electronic structures of hexagonal CrB_4 sheet

Jinkun Wang(王锦坤), Yajiao Ke(柯亚娇), Qingxing Xie(谢晴兴), Yanli Li(李艳丽), Jiafu Wang(王嘉赋)
Chin. Phys. B . 2018, 27(9): 097304. **doi:** 10.1088/1674-1056/27/9/097304

First-principles modeling hydrogenation of bilayered boron nitride

Jing Wang(王静), Peng Zhang(张鹏), Xiang-Mei Duan(段香梅)
Chin. Phys. B . 2016, 25(5): 057301. **doi:** 10.1088/1674-1056/25/5/057301

Silicene on substrates: A theoretical perspective

Zhong Hong-Xia, Quhe Ru-Ge, Wang Yang-Yang, Shi Jun-Jie, Lü Jin
Chin. Phys. B . 2015, 24(8): 087308. **doi:** 10.1088/1674-1056/24/8/087308

Lattice structures and electronic properties of CIGS/CdS interface：First-principles calculations

Tang Fu-Ling, Liu Ran, Xue Hong-Tao, Lu Wen-Jiang, Feng Yu-Dong, Rui Zhi-Yuan, Huang Min
Chin. Phys. B . 2014, 23(7): 077301. **doi:** 10.1088/1674-1056/23/7/077301

Optimized geometry and electronic structure of graphyne-like silicyne nanoribbons

Pei Yang, Wu Hai-Bin
Chin. Phys. B . 2013, 22(5): 057303. **doi:** 10.1088/1674-1056/22/5/057303

Hydrogenated antimonene as quantum spin Hall insulator: A first-principles study*

Xin He(贺欣)[1,2,†] and Ji-Biao Li(李佶彪)[3]

[1] School of Intelligent Manufacturing, Sichuan University of Arts and Science, Dazhou 635000, China
[2] Dazhou Industrial Technology Institute of Intelligent Manufacturing, Dazhou 635000, China
[3] Chongqing Key Laboratory Bond Engineering and Advanced Materials Technology (EBEAM), Yangtze Normal University, Chongqing 408100, China

(Received 10 September 2018; revised manuscript received 15 January 2019; published online 22 February 2019)

Using first-principles calculations based on density functional theory (DFT), the structural and electronic properties of hydrogenated antimonene have been systematically investigated. Phonon dispersion and molecular dynamics (MD) simulation reveal that fully hydrogenated (FH) antimonene has high dynamic stability and could be synthesized. A new σ-type Dirac cone related to Sb-$p_{x,y}$ orbitals is found in FH antimonene, which is robust to tensile strain. Noticeably, the spin orbital coupling (SOC) opens a quantum spin Hall (QSH) gap of 425 meV at the Dirac cone, sufficiently large for practical applications at room temperature. Semi-hydrogenated antimonene is a non-magnetic metal. Our results show that FH antimonene may have great potential applications in next generation high-performance devices.

Keywords: antimonene, Dirac cone, quantum spin Hall (QSH) insulator, hydrogenated, first-principles calculations

PACS: 73.20.At, 71.15.Mb, 71.20.Mq **DOI:** 10.1088/1674-1056/28/3/037301

1. Introduction

Since graphene was first isolated through mechanical exfoliation from ghaphite sheets in 2004,[1] two-dimensional (2D) materials such as transition metal dichacogenides, silicene, germanene, stananene, and phosphenene have been extensively studied[2,3] over the past decade. Owing to the unique honeycomb structure, 2D materials exhibit extraordinary properties, including topological insulator effect,[4] superconductivity,[5] and thermoelectricity,[6] which make them attractive for a wide range of applications in spintronics, optoelectronics, chemical sensors, and energy conversion or storage.[2,7,8] Recently, two novel graphene-like 2D materials, namely asenene and antimonene, were predicted through first-principles calculations by Zhang *et al*.[9] As the analogues of black phosphenene, asenene and antimonene have wide band gaps and high stability. To achieve multifunctional devices, it is crucial to tune the structural, electronic, and magnetic properties of 2D materials by various methods, including strain,[10] doping,[11,12] chemical functionalization,[13] and external electric field,[14] among which the chemical functionalization is an extremely effective way because of its high chemical reactivity.

Up to now, it has been reported that fully hydrogenated arsenene is a Dirac material and semi-hydrogenated arsenene exhibits significant magnetism.[15] Moreover, fully halogenated arsenene[16] and chemically decorated arsenene, AsX (X = CN, NC, NCO, NCS, and NCSe),[17] were also found to be Dirac materials. However, as far as we know, functionalized antimonene has not been reported till now. In this work, we investigate the structural and electronic properties of fully hydrogenated (FH) antimonene and semi-hydrogenated (SH) antimonene using first-principles calculations.

2. Method

First-principles calculations are performed within the framework of density functional theory (DFT) implemented in Quantum ESPRESSO package[18,19] using a norm-conserving pseudopotentials[20] and fully-relativistic ultrasoft pseudopotentials[21] for calculations without spin–orbital coupling (SOC) calculations and with SOC calculations, respectively. Spin polarization is included throughout the calculation. The exchange–correlation functional is treated using generalized-gradient approximation (GGA) of Perdew–Burke–Eruzerhof (PBE).[22] The unit cell optimization is terminated upon reaching the pressure cut-off of 0.01 kbar. The energy cutoff of the plane waves is set to 150 Ry in all computations except molecular dynamics (MD) simulation and nanoribbon. The energy criterion is set to 10^{-10} Ry for both electronic self consistency and structural optimization. A 20 Å vacuum layer is used to simulate the isolated sheet. The Brillouin zone integration is represented by the Monkhorst–Pack k-point scheme[23] with $15 \times 15 \times 1$ grid mesh. All the lattice constants and atom coordinates are optimized until the convergence of the force on each atom is less than 10^{-5} Ry/bohr. The SOC is included in the self-consistent calculations of electronic structure. Phonon dispersion is ob-

*Project supported by Research Funds of Sichuan University of Arts and Science, China (Grant No. 2012Z009Y).
†Corresponding author. E-mail: 18398818113@163.com
© 2019 Chinese Physical Society and IOP Publishing Ltd

tained by lattice dynamic calculations performed using density functional perturbation theory[24] within linear response approach and by using the small displacement method[25] for antimonene and hydrogenated antimonene, respectively. First-principles MD simulation is performed with a canonical (NVT) ensemble. The simulation time step is 1 fs and the simulation time is 1 ps. The 4×4 supercell containing 64 atoms is equilibrated at 300 K. The energy cutoff of the plane waves is set to 40 Ry in MD simulation and for nanoribbon.

3. Results and discussion

Figure 1 shows the optimized crystal structures of pristine antimonene, fully hydrogenated antimonene, and semi-hydrogenated antimonene with the Sb–Sb bond length and buckling height. The key structural parameters are summarized in Table 1. We first check the equilibrium configuration of pristine antimonene. The calculated lattice constant, Sb–Sb bond length, and bond angle are 4.11 Å, 2.88 Å, and 91°, respectively, which agrees well with the previous work.[9] As can be seen, pristine antimonene has a buckled honeycomb-like structure with a buckling height of 1.64 Å, which is mainly attributed to the mixing of sp^2 and sp^3 hybridizations. After semi-hydrogenation, the buckling height decreases to 0.91 Å and the corresponding bond angle increases to 110.75°. Moreover, the buckling height of fully hydrogenated antimonene is dramatically decreased to 0.08 Å and results in the almost qusi-planar configurations with the bond angle of approximately 120°, indicating that a bonding is nearly an ideal sp^2 character. The Sb–H bond is 1.723 Å and 1.726 Å for semi-hydrogenated and fully hydrogenated antimonene, respectively, which reveals that hydrogen atoms are chemically absorbed in antimonene sheet. From our calculations, both the semi-hydrogenated and fully hydrogenated antimonene are nonmagnetic, though other semi-hydrogenated analogues of antimonene have been reported to be ferromagnetic.[15,26,27]

Table 1. Structural parameters calculated for pristine antimonene, fully hydrogenated antimonene, and semi-hydrogenated antimonene. Lattice constants a, buckling height Δ, bond angle θ, Sb–Sb bond length $l_{\mathrm{Sb-Sb}}$, and Sb–H bond length $l_{\mathrm{Sb-H}}$ are given.

	a/Å	Δ/Å	θ/(°)	$l_{\mathrm{Sb-Sb}}$/Å	$l_{\mathrm{Sb-H}}$/Å
Sb	4.11	1.64	91.00	2.88	–
FH-Sb	5.27	0.08	119.92	3.04	1.723
SH-Sb	4.83	0.91	110.75	2.93	1.726

To verify the structural stability of pristine antimonene and hydrogenated antimonene, we perform phonon dispersion calculations. Figures 2(a) and 2(b) show the phonon dispersion along the highly symmetric points in the Brillouin zone of pristine antimonene and FH antimonene. Both the phonon spectra do not have imaginary frequencies, which means they own high stability. Moreover, we carry out first-principles MD simulations in canonical ensemble to examine the thermal stability of the FH antimonene at room temperature. A 4×4 supercell containing 64 atoms is used and MD simulation is performed at $T = 300$ K. Figure 2(c) shows the snapshot of FH antimonene taken at 1 ps. It can be clearly seen that the framework of FH antimonene is well kept as its initial equilibrium structure at $T = 300$ K. As we know, free-standing antimonene has been obtained in the experiment.[28] Our results indicate that FH antimonene has highly dynamic stability even at room temperature, and could also be synthesized in the experiment in the future.

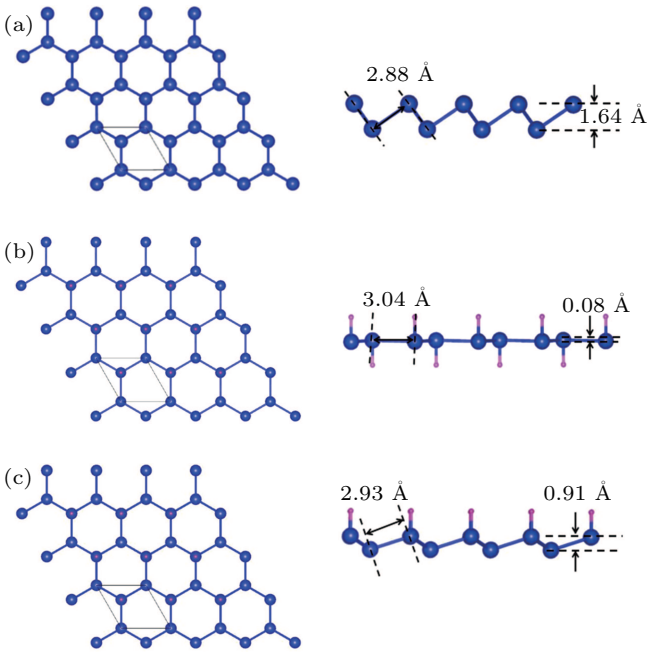


Fig. 1. Top view (left) and side view (right) of optimized (a) pristine antimonene, (b) fully hydrogenated antimonene, and (c) semi-hydrogenated antimonene.

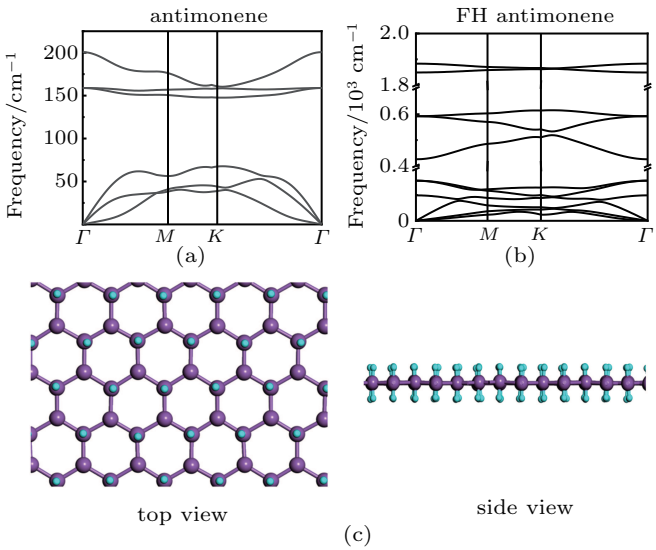


Fig. 2. Phonon band dispersions of (a) pristine antimonene and (b) FH antimonene. (c) Snapshot of FH antimonene structure in MD simulation at 300 K after 1 ps.

Antimonene is a semiconductor with an indirect band gap of 1.24 eV in our calculations. The band structure with and without SOC and the corresponding total density of states (TDOS) and projected density of states (PDOS) of FH and SH antimonene are presented in Fig. 3. For FH antimonene without SOC, it is found that two energy bands cross linearly at the K point, forming an obvious Dirac cone that lies exactly at the Fermi level. The linear dispersion indicates that the carriers in FH antimonene are massless Dirac fermion. According to linear spectrum $E = \hbar v_{\mathrm{F}} k$, Fermi velocities v_{F} of FH antimonene is calculated to be in the order of 10^6 m/s, indicating an excellent electronic transport feature. A sizeable band gap of 425 meV opens up at Dirac cone when the SOC is turned on. Thus, FH antimonene is a quantum spin Hall (QSH) insulator, which was first proposed by Kane and Mele in graphene.[29] Because the space inversion symmetry is present in FH antimonene, the Z_2 invariant can be calculated following the parity method proposed by Fu and Kane.[30] We find the Z_2 of FH antimonene is 1, indicating that it is a QSH insulator, which is similar to some other systems.[31,32] While for SH antimonene, it exhibits a typical metallic character with a band across the Fermi level. In order to analyze the origin of Dirac cone in FH antimonene, the corresponding TDOS and PDOS are calculated. It is evident that the Dirac cone originates from the Sb-p orbital. As a matter of fact, the Sb atom has five valence electrons. It is assumed that three of them form the covalent σ bonds with three Sb atoms, while another one is saturated by hydrogen atom, leaving an extra unbonded electron. Obviously, this yields a graphene-like structure which only has sp^2 hybridization. This can be further verified by projecting the component of bands of FH antimonene. From Fig. 4, it can be seen that Dirac cone mainly comes from Sb-$p_{x,y}$ orbitals, as illustrated by the size of circles near the Fermi level. In this case, it is the Sb-$p_{x,y}$ orbitals that form σ bonds between Sb–Sb atoms, demonstrating an in-plane Dirac cone feature. Such Dirac states composed of $p_{x,y}$ orbitals are refered to as σ-type Dirac cone, which has been reported in several 2D systems including fluoridated tin films and functionalized germanene.[33,34] From Fig. 3(b), in the energy region $(-1, 1)$ eV, the contribution to TDOS mainly comes from p obital of Sb atom, indicating that the conduction band is mainly attributed to p orbital of Sb atom.

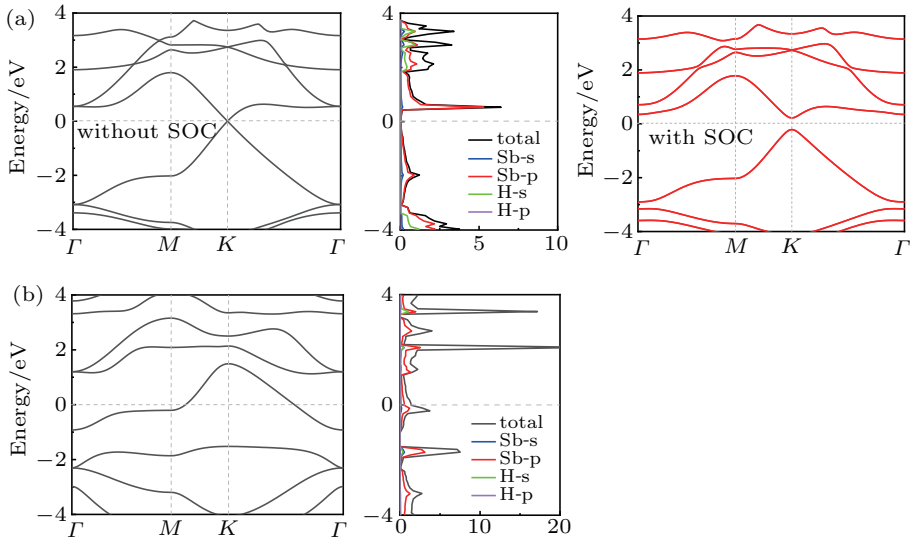


Fig. 3. Band structure with and without SOC and the corresponding TDOS and PDOS of (a) FH and (b) SH antimonene.

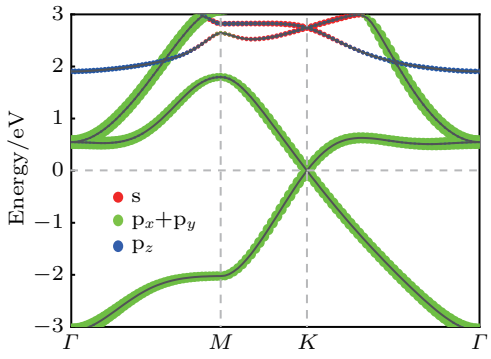


Fig. 4. Projected band structure of FH antimonene with contribution from s, p_x+p_y, and p_z orbitals represented by red, green, and blue dots, respectively.

One of the prominent features of QSH insulators is the existence of gapless edge states that are helical with the spin-momentum locked. In order to explicitly demonstrate the edge states for FH antimonene, a zigzag nanoribbon (ZNR) with space inversion symmetry is constructed with the edges passivated by hydrogen atoms, as shown in Fig. 5(a). For avoiding interaction between the edge states, FH antimonene ZNR with width of $N = 7$ (3.24 nm) is selected, where N is classified by the number of zigzag chains across the ribbon width. The calculated bandstructure of FH antimonene ZNR is presented in Fig. 5(b). We can clearly see one pair of helical edge states cross at the X point, exhibiting the topological nontrivial prop-

erty. Figure 5(c) shows the localized density of states (LDOS) plots of ZNR of FH antimonene. As expected, ZNR of FH antimonene are metallic and the density of states (DOS) near the Fermi level is mainly attributed to edge atoms. The charge density distribution of edge states near the Fermi level is depicted in Fig. 5(d), which clearly shows that they are localized along the edge of the ribbon. All the above results consistently indicate that FH antimonene is a QSH insulator.

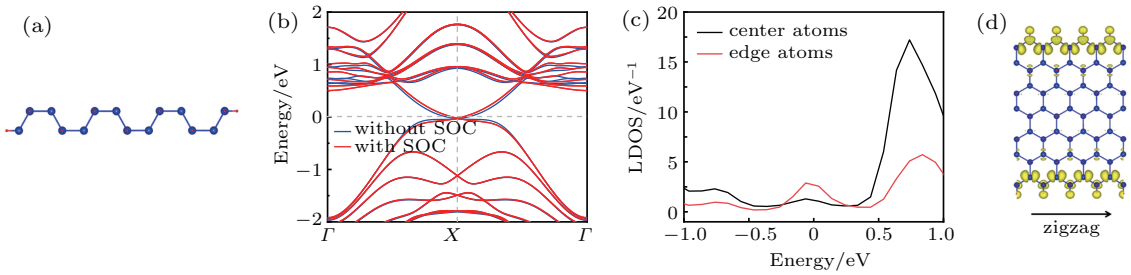


Fig. 5. (a) Top view of zigzag nanoribbon of FH antimonene with width of $N = 7$ (3.24 nm). (b) Band structure of ZNR for FH antimonene with (red) and without (blue) SOC. (c) The LDOS plots of ZNR. (d) Charge density distribuion in real space of the edge state near Fermi level.

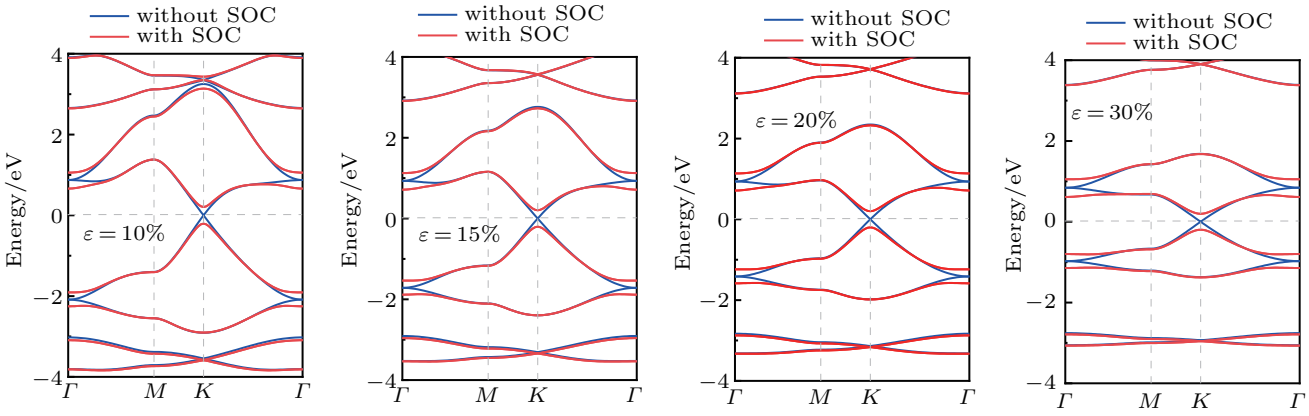


Fig. 6. Band structure of FH antimonene without (blue) and with (red) SOC under different biaxial strain.

To see what would happen to Dirac cone in FH antimonene when the in-plane tensile strain is applied, we investigate the structural and electronic properties of FH antimonene under a biaxial strain. Here, a biaxial strain is defined as $\varepsilon = (a - a_0)/a_0$, where a and a_0 are the lattice constants of the strained and the equilibrium unit, respectively. The band structure of FH antimonene with and without SOC under different strains are shown in Fig. 6. We can see that Dirac cone in FH antimonene without SOC still exits even under 30% biaxial strain. And in all cases, band gap opens at Dirac cone when SOC is turned on. It means that FH antimonene as a QSH insulator is robust to tensile strain, which provides a good reference for the design of future nanoelectronic devices.

4. Conclusion

In summary, we have explored the hydrogenated antimonene by first-principles calculations. FH antimonene is a QSH insulator with a band gap of 425 meV. Moreover, FH antimonene has high dynamic stability even at room temperature, indicating that it could be obtained in experiments. We have revealed that Dirac cone in FH antimonene is related to Sb-$p_{x,y}$ orbitals, which is robust to tensile strain. SH antimonene is found to be a non-magnetic metal. We expect the experimental realization of FH antimonene and its great potential in next-generation high-performance devices.

Acknowledgment

We thank Dr. Botao Fu for help of calculating Z_2 invariant. Dr. Shangyi Ma is acknowledged for discussion on MD simulations.

References

[1] Novoselov K S, Geim A K, Morozov S V, Jiang D, Zhang Y, Dubonos S V, Grigorieva I V and Firsov A A 2004 *Science* **306** 666
[2] Wang Q H, Kalantar-Zadeh K, Kis A, Coleman J N and Strano M S 2012 *Nat. Nanotechnol.* **7** 699
[3] Balendhran S, Walia S, Nili H, Sriram S and Bhaskaran M 2015 *Small* **11** 640
[4] Saxena S, Chaudhary R P and Shukla S 2016 *Sci. Rep.* **6** 31073
[5] Pan J, Guo C G, Song C S, Lai X F, Li H, Zhao W, Zhang H, Mu G, Bu K J, Lin T Q, Xie X M, Chen M W and Huang F Q 2017 *J. Am. Chem. Soc.* **139** 4623
[6] Wang F Q, Zhang S H, Yu J B and Wang Q 2015 *Nanoscale* **7** 15962
[7] Pumera M 2011 *Energy Environ. Sci.* **4** 668
[8] Liu Y X, Dong X C and Chen P 2012 *Chem. Soc. Rev.* **41** 2283
[9] Zhang S L, Yan Z, Li Y F, Chen Z F and Zeng H B 2015 *Angew. Chem.* **127** 3155
[10] Castellanos-Gomez A, Roldán R, Cappelluti E, Buscema M, Guinea F, van der Zant H S J and Steele G A 2013 *Nano Lett.* **13** 5361
[11] Cheng Y C, Zhu Z Y, Mi W B, Guo Z B and Schwingenschlögl U 2013 *Phy. Rev. B* **87** 100401(R)

[12] Wang J Z, Yang T, Zhang Z D and Yang L 2018 *Appl. Phys. Lett.* **112** 213104
[13] Tang Q, Zhou Z and Chen Z F 2013 *Nanoscale* **5** 4541
[14] Liu Q H, Zhang X W, Abdalla L B, Fazzio A and Zunger A 2015 *Nano Lett.* **15** 1222
[15] Zhang S L, Hu Y H, Hu Z Y, Cai B and Zeng H B 2015 *Appl. Phys. Lett.* **107** 022102
[16] Tang W C, Sun M L, Ren Q Q, Wang S K and Yu J 2016 *Appl. Surf. Sci.* **376** 286
[17] Yuan J H, Xie Q X, Yu N N and Wang J F 2017 *Appl. Surf. Sci.* **394** 625
[18] Giannozzi P, Baroni S, Bonini N, *et al.* 2009 *J. Phys: Condens. Matter* **21** 395502
[19] Giannozzi P, Andreussi O, Brumme T, *et al.* 2017 *J. Phys: Condens. Matter* **29** 465901
[20] Hamann D R, Schlüter M and Chiang C 1979 *Phys. Rev. Lett.* **43** 1494
[21] Dal Corso A and Conte A M 2005 *Phys. Rev. B* **71** 115106
[22] Perdew J P, Burke K and Ernzerhof M 1996 *Phys. Rev. Lett.* **77** 3865
[23] Monkhorst H J and Pack J D 1976 *Phys. Rev. B* **13** 5188
[24] Baroni S, De Gironcoli S, Dal Corso A and Giannozzi P 2001 *Rev. Mod. Phys.* **73** 515
[25] Kunc K and Martin R M 1982 *Phys. Rev. Lett.* **48** 406
[26] Wang X Q, Li H D and Wang J T 2012 *Phys. Chem. Chem. Phys.* **14** 3031
[27] Li S S and Zhang C W 2016 *Mater. Chem. Phys.* **173** 246
[28] Ares P, Aguilar-Galindo F, Rodríguez-San-Miguel D, Aldave D A, Díaz-Tendero S, Alcamí M, Martín F, Gómez-Herrero J and Zamora F 2016 *Adv. Mater.* **28** 6332
[29] Kane C L and Mele E J 2005 *Phys. Rev. Lett.* **95** 226801
[30] Fu L and Kane C L 2007 *Phys. Rev. B* **76** 045302
[31] Zhang Q Y and Schwingenschlögl U 2016 *Phys. Rev. B* **93** 045312
[32] Fu B T, Ge Y F, Su W Y, Guo W and Liu C C 2016 *Sci. Rep.* **6** 30003
[33] Xu Y, Yan B H, Zhang H J, Wang J, Xu G, Tang P Z, Duan W H and Zhang S C 2013 *Phys. Rev. Lett.* **111** 136804
[34] Si C, Liu J W, Xu Y, Wu J, Gu B L and Duan W H 2014 *Phys. Rev. B* **89** 115429